# Spacecraft Attitude Control with Precise Pointing the Flexible Antennas*

**Ye. I. Somov** [*], **G. P. Titov** [†], **and Ye. N. Yakimov** [†]

[*] *Samara Scientific Center, Russian Academy of Sciences (RAS), 3a Studenchesky Lane, Samara 443001 Russia (e-mail: e_somov@mail.ru)*

[†] *JSC "Acad. Reshetnev Information Satellite Systems" Company (ISS Reshetnev), Federal Space Agency (FSA), 52 Lenin Str., Zheleznogorsk 662972 Russia (e-mail: titov@iss-reshetnev.ru)*

**Abstract:** New approach for modelling a physical hysteresis damping the flexible spacecraft structure oscillations, is developed. New results on communication satellite attitude guidance and digital robust control with precise pointing the large-scale flexible antennas, are presented.

*Keywords:* communication satellite, attitude control, flexible antenna, pointing

## 1. INTRODUCTION

A correct mathematical description of physical hysteresis is a basic problem for an internal friction theory (N.N. Davidenkov, 1938; A.Yu. Ishlinskii, 1944; W. Prager, 1956; J.F. Besseling, 1958; Ye.S. Sorokin, 1960; Ya.G. Panovko (1960); G.S. Pisarenko (1970); V.A. Palmov (1976); L.F. Kochneva (1979) et al.) with regard to the well-known elastico-plastic micro-deformations of materials. Mathematical methods for qualitative analysis of general hysteresis models are represented in a number of research works (Krasnosel'skii and Pokrovskii, 1983). Recently, new approach was developed for description of physical hysteresis (Somov, 2000, 2004), which is based on set-valued differential equation with discontinuous right-side. The paper briefly presents new results on modelling a hysteresis damping and their application to the attitude guidance and robust digital control of large-scale communication spacecraft (SC) with precise pointing the flexible weak-damping antennas.

## 2. MODEL OF PHYSICAL HYSTERESIS

Let $x(t)$ is a real piecewise-differetiated function for $t \in \mathrm{T}_{t_0} \equiv [t_0, +\infty)$. Let there be the values $\check{x}_\nu = x(t_\nu)$ of the function in the time moments $t_\nu$, $\nu \in \mathbb{N}_0 \equiv [0, 1, 2, \cdots)$, when the *last* changing a *sign* of a speed $\dot{x}(t)$ was happened, e.g.

$$\check{x}_\nu \equiv x(t_\nu)|_{t_\nu:\mathrm{Sign}\dot{x}(t_\nu+0)\neq\mathrm{Sign}\dot{x}(t_\nu-0)}. \qquad (1)$$

A *local* function $\tilde{x}_\nu(t)$ on each a local time semi-interval $\mathrm{T}_\nu \equiv [t_\nu, t_{\nu+1})$ is introduced as

$$\tilde{x}_\nu(t) = x(t) - \check{x}_\nu \quad \forall t \in \mathrm{T}_\nu, \qquad (2)$$

and the functional $k_\nu(x(t)) \equiv k_\nu(k, p, \tilde{p}, \tilde{x}_\nu)$ of the hysteresis function *shape* is defined for $t \in \mathrm{T}_\nu$ as

$$k_\nu(x(t)) = k(1 - (1-p)\exp(-\tilde{p}|\tilde{x}_\nu|)), \qquad (3)$$

where $k, p, \tilde{p}$ are constant positive parameters.

* The work was supported by RFBR (Grant 08-08-00512) and by Division on EMMCP of the RAS (Program 15).

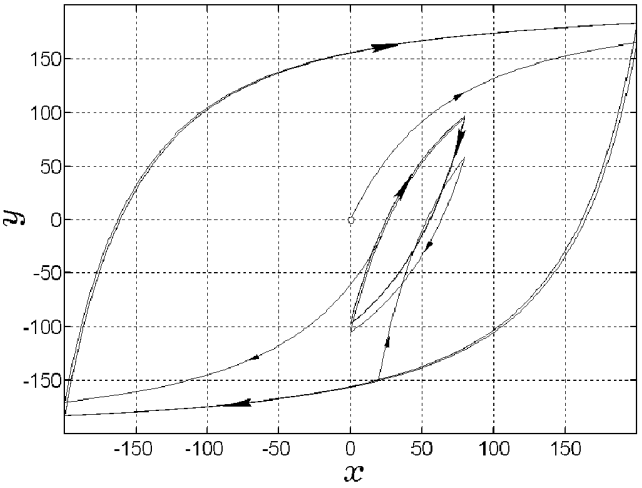


Fig. 1. Results of a hysteresis model testing

For a constant parameter $\alpha_h > 0$ and $x_0 \equiv x(t_0)$ a *normed* hysteresis function $r(t) = \mathrm{Hst}(\cdot, x(t))$ with memory

$$\begin{aligned} r(t) &= \mathrm{Hst}(a_h, \alpha_h, k_\nu(x(t)), r_o, x(t)); \\ r(t_0) &\equiv r_o = \mathrm{Hst}(a_h, \alpha_h, k_\nu(x_0), r_o, x_0) \end{aligned} \qquad (4)$$

and restriction on its module by parameter $a_h > 0$, is defined as a right-sided solution of the equations

$$\mathrm{D}^+ r = \begin{cases} k_\nu \, |r - a_h \mathrm{Sign}\, \dot{x}(t)|^{\alpha_h} \, \dot{x}(t) & |r| < a_h \\ 0 & |r| \geq a_h \end{cases}; \qquad (5)$$
$$r(t_0 + 0) = r_o.$$

Differential equation in (5) has a discontinuous right side and ambiquitely depends on forcing function $x(t)$ and its speed $\dot{x}(t)$, e.g. it depends on all own prehistory which is expressed by the functional $k_\nu(x)$ (3). At initial condition $y_o \equiv y_0 = y(t_0)$ for $x = x_0$ the hysteresis function $y(t)$ is defined as follows

$$y(t) \equiv m \, \mathrm{Hst}(a_h, \alpha_h, k_\nu, r_o, x(t)); \quad r_o \equiv y_o/m \qquad (6)$$

with a constant positive scale coefficient $m > 0$. In developed model (1) – (6) a parameter $\tilde{p}$ determines on the

whole a degree of convergence for a trajectory $y(t) = F_h(\cdot, x(t))$ in the plane $x\mathrm{O}y$ on symmetric limiting static loop under a harmonic forcing function $x(t) = A\sin\omega t$ with fixed values $A, \omega$ and initial condition $y_o = y_0$ with $|y_o|/m < a_h$. For this model all requirements are realized, including the famous requirements on a model vibro-correctness by M.A. Krasnosel'skii (Krasnosel'skii and Pokrovskii, 1983), and also on a frequency independence and a fine return on a main symmetric limiting hysteresis loop after a short-term passage on a displaced local hysteresis loop (Palmov, 1976; Kochneva, 1979). Last properties are verified in prearranged scale by Fig. 1 for the hysteresis model with parameters $m=1$, $\alpha_h=1.5, a_h=200, k=5.125\,10^{-4}, p=2$, $\tilde{p}=0.75\,10^{-3}$ when the forcing function have the form:

$$x(t)=\begin{cases} A\sin\omega_1 t & (0\le t<\tau_1)\&(\tau_2\le t\le\tau_3);\\ B(1+\sin\omega_2 t) & \tau_1\le t<\tau_2,\end{cases}$$
$$A=200;\ B=40;\ \omega_1=1;\ \omega_2=5;\ \tau_3=40;$$
$$\tau_1\equiv 5\pi-\tau^*;\ \tau_2=7\pi-\tau^*;\ \tau^*\approx 0.03415\pi.$$

## 3. MATHEMATICAL MODELS

We introduce the inertial reference frame (IRF) $\mathbf{I}_\oplus$, the geodesic Greenwich reference frame (GRF) $\mathbf{E}_\mathrm{e}$ and the geodesic horizon reference frame (HRF) $\mathbf{E}^\mathrm{h}_\mathrm{e}$. There are also standard defined the SC body reference frame (BRF) $\mathbf{B}$ ($\mathrm{O}xyz$), the orbit reference frame (ORF) $\mathbf{O}$ ($\mathrm{O}x^\mathrm{o}y^\mathrm{o}z^\mathrm{o}$) and the antenna (sensor) reference frame (SRF) $\boldsymbol{\mathcal{S}}$ ($\mathrm{S}x^\mathrm{s}y^\mathrm{s}z^\mathrm{s}$) with an origin S. The BRF attitude with respect to the IRF $\mathbf{I}_\oplus$ is defined by quaternion $\boldsymbol{\Lambda}=(\lambda_0,\boldsymbol{\lambda}), \boldsymbol{\lambda}=(\lambda_1,\lambda_2,\lambda_3)$, and with respect to the ORF – by column $\boldsymbol{\phi}=\{\phi_i, i=1\div 3\}$ of angles $\phi_1=\psi, \phi_2=\varphi, \phi_3=\theta$ in the sequence $13'2''$.

Let vectors $\boldsymbol{\omega}(t)$ and $\mathbf{v}(t)$ are standard denotations of the SC body angular rate and its mass center velocity with respect to the IRF, respectively, and vector $\mathbf{v}_\delta(t)$ presents the $\mathbf{v}(t)$ deviation with respect to nominal SC orbital motion at the Earth gravity field. Applied further symbols $\langle\cdot,\cdot\rangle$, $\times$, $\{\,\cdot\,\}$, $[\,\cdot\,]$ for vectors and $[\mathbf{a}\times]$, $(\cdot)^\mathrm{t}$ for matrixes are conventional denotations. For a fixed position of flexible structures on the SC body with some simplifying assumptions and $t\in \mathrm{T}_{t_0}=[t_0,+\infty)$ model of the SC spatial motion is appeared as follows:

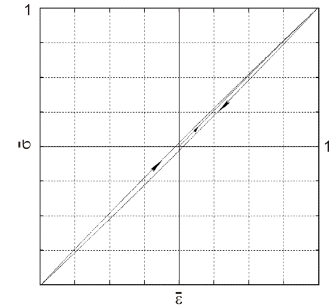

Fig. 2. A normed hysteresis

$$\dot{\boldsymbol{\Lambda}}=\boldsymbol{\Lambda}\circ\boldsymbol{\omega}/2;\ \mathbf{A}^\mathrm{o}\{\overset{*}{\mathbf{v}}_\delta,\dot{\boldsymbol{\omega}},\ddot{\mathbf{q}},\ddot{\boldsymbol{\beta}}\}=\{\mathbf{F}^\mathrm{v}_\delta,\mathbf{F}^\omega,\mathbf{F}^q,\mathbf{F}^\beta\};\quad (7)$$
$$\mathbf{F}^\mathrm{v}_\delta=-\mathrm{m}(\boldsymbol{\omega}\times\mathbf{v}_\delta)+\boldsymbol{\omega}\times(\mathbf{L}\times\boldsymbol{\omega}-2\dot{\mathbf{L}})+\mathbf{R}^\mathrm{c};\ \mathbf{L}=\mathbf{M}_q\mathbf{q};$$
$$\mathbf{F}^\omega=-\mathbf{L}\times(\boldsymbol{\omega}\times\mathbf{v}_\delta)+\mathbf{M}^\mathbf{g}-\boldsymbol{\omega}\times\mathbf{G}+\mathbf{M}^\mathrm{o};\mathbf{M}^\mathbf{g}=-\mathbf{A}_\mathrm{h}\dot{\boldsymbol{\beta}};$$
$$\mathbf{F}^q=\{-(\Omega^q_j)^2 m_j r_j(t)\};\qquad \mathbf{F}^\beta=\mathbf{A}^\mathrm{t}_\mathrm{h}\boldsymbol{\omega}+\mathbf{M}^g+\mathbf{M}^q_d+\mathbf{M}^g_f;$$
$$r_j(t)=\mathrm{Hst}(a^j_h,\alpha^j_h,k^j_\nu(x_j),x_{oj},x_j(t));\quad x_j(t)=q_j(t)/m_j;$$
$$\mathbf{A}^\mathrm{o}=\begin{bmatrix}\mathrm{m}\mathbf{I}_3 & [-\mathbf{L}\times] & \mathbf{M}_q & \mathbf{0}\\ [\mathbf{L}\times] & \mathbf{J} & \mathbf{D}_q & \mathbf{D}_g\\ \mathbf{M}^\mathrm{t}_q & \mathbf{D}^\mathrm{t}_q & \mathbf{I} & \mathbf{0}\\ \mathbf{0} & \mathbf{D}^\mathrm{t}_g & \mathbf{0} & \mathbf{A}^g\end{bmatrix};$$
$$\mathbf{G}=\mathbf{G}^o+\mathbf{D}_q\dot{\mathbf{q}}+\mathbf{D}_g\dot{\boldsymbol{\beta}};\ \mathbf{G}^o=\mathbf{J}\boldsymbol{\omega}+\boldsymbol{\mathcal{H}}(\boldsymbol{\beta});\ \boldsymbol{\omega}=\{\omega_i\};$$
$$\boldsymbol{\mathcal{H}}(\boldsymbol{\beta})=\Sigma\mathbf{H}_p=\mathrm{h}_g\Sigma\mathbf{h}_p(\beta_p);\mathbf{A}_\mathrm{h}=[\partial\boldsymbol{\mathcal{H}}(\boldsymbol{\beta})/\partial\boldsymbol{\beta}];\boldsymbol{\beta}=\{\beta_p\},$$

where $\mathrm{h}_g$ is a constant own angular momentum (AM) of each gyrodine (GD) and $x_{oj}=q_j(t_0)/m_j$ by conditions (6). Parameters $m_j$, $a^j_h$, $\alpha^j_h$, $k_j, p_j, \tilde{p}_j$ by functionals $\mathrm{Hst}(\cdot)$ and $k^j_\nu$ for tones of the SC structure oscillations are defined by an identification starting from analysis of experimental hysteresis loop for normed mechanical deformation $\bar{\varepsilon}$ and strength $\bar{\sigma}$ of the structure material, see Fig. 2.

At standard linear modelling one can have

$$\mathbf{F}^q=\{-((\delta^q_j/\pi)\,\Omega^q_j\,\dot{q}_j+(\Omega^q_j)^2\,q_j)\},\qquad (8)$$

where $\delta^q_j\in[10^{-3},\,2\,10^{-4}]$ is decrement by $j$-tone of the SC structure flexible oscillations. The antenna's flexibility results in additional angular deflection of the SRF $\boldsymbol{\mathcal{S}}$ with respect its nominal position in the BRF, including its line-of-sight $\mathrm{S}x^\mathrm{s}$. The deflection is presented by column $\delta\boldsymbol{\phi}\equiv\{\delta\phi_i, i=1\div 3\}$ of the angels $\delta\phi_i$ as follows

$$\delta\boldsymbol{\phi}=\mathbf{Q}_q\,\mathbf{q},\qquad (9)$$

where matrix $\mathbf{Q}_q$ is calculated by the antenna's shape modes.

The torque column $\mathbf{M}^g_d$ of physical and electro-magnetic damping is nonlinear continuous function, and column $\mathbf{M}^g_f$ of the rolling friction torques in bearings on GD's precession axes is *discontinuous* vector-function. The gyro moment cluster (GMC) control vector $\mathbf{M}^g(t)=\{\mathrm{m}^g_p(t)\}$ have components which are described by relation

$$\mathrm{m}^g_p(t)=a^g\,\mathrm{Zh}[\mathrm{Sat}(\mathrm{Qntr}(u^g_{pk},b_u),B_u),\mathrm{T}_u];k\in\mathbb{N}_0,\quad (10)$$

where $\mathbb{N}_0\equiv[0,1,2,...)$, $a^g=\mathrm{const}$, discrete functions $u^g_{pk}\equiv u^g_p(t_k)$ are outputs of nonlinear control law, and functions $\mathrm{Sat}(x,a)$ and $\mathrm{Qntr}(x,a)$ are general-usage ones, while the holder model with the period $\mathrm{T}_u$ is of the type: $y(t)=\mathrm{Zh}[x_k,\mathrm{T}_u]=x_k\quad \forall t\in[t_k,t_{k+1})$. Model (7),(10) is applied then the GD driver have *small* gear ratio, e.g. for "soft" gyromoment control where the *nutation theory* must be used.

For the GD driver gear with *large* transfer ratio the command $\mathrm{u}^\mathrm{g}_p=\dot{\beta}^\mathrm{c}_p(t)$ and the true $\dot{\beta}_p(t)$ precession rates are close. Then the assumptions of the control moment gyros *precession theory* are satisfied, and the vector $\mathbf{M}^\mathbf{g}=\{\mathrm{M}^\mathrm{g}_i\}$ of the GMC output control torque is presented by relation

$$\mathbf{M}^\mathbf{g}=-\overset{*}{\boldsymbol{\mathcal{H}}}=-\mathbf{A}_\mathrm{h}(\boldsymbol{\beta})\,\mathbf{u}^\mathrm{g}(t);\ \dot{\boldsymbol{\beta}}=\mathbf{u}^\mathrm{g}(t)\equiv\{\mathrm{u}^\mathrm{g}_p(t)\},\quad (11)$$

where $\mathrm{u}^\mathrm{g}_p(t)=a^\mathrm{g}\,\mathrm{Zh}[\mathrm{Sat}(\mathrm{Qntr}(u^g_{pk},b_u),B_u),\mathrm{T}_u]$ with a constant $a^\mathrm{g}$. Moreover matrix $\mathbf{D}_g=\mathbf{0}$, last vector equation in model (7) must be rejected and one can to obtain so-called "stiff" gyromoment control.

## 4. THE PROBLEM STATEMENT

Applied onboard measuring subsystem is based on a precise gyro unit corrected by the fine fixed-head star trackers. This subsystem is intended for precise determination of the SC BRF $\mathbf{B}$ angular position with respect to the IRF $\mathbf{I}_\oplus$. Applied contemporary filtering & alignment calibration algorithms and a discrete astatic observer give finally a fine discrete estimating the SC angular motion coordinates presented by the quaternion estimation $\hat{\boldsymbol{\Lambda}}_s$ and the angular rate estimation $\hat{\boldsymbol{\omega}}_s$, where $s\in\mathbb{N}_0$ and a measuring period

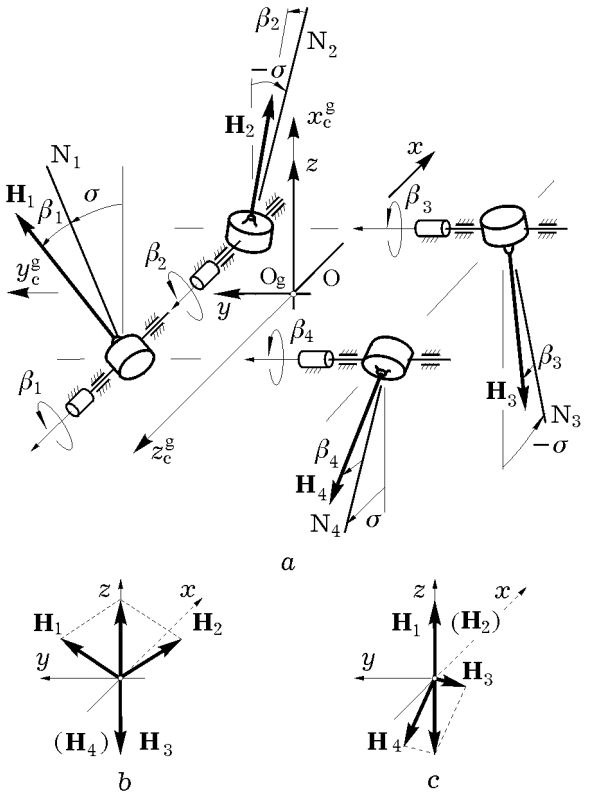


Fig. 3. The fault-tolerant *2-SPE* scheme of the GMC

$T_q = t_{s+1} - t_s \le T_u$ is multiply with respect to a control period $T_u$.

Applied the *2-SPE* scheme on 4 GDs with the AM vectors $\mathbf{H}_p, p = 1 \div 4$ is presented in Fig. 3 (Somov et al., 2005b,a). Into canonical reference frame $\mathrm{O_g}x_c^{\mathrm{g}}y_c^{\mathrm{g}}z_c^{\mathrm{g}}$ of the gyro moment cluster (GMC) the AM projections of the first (GD-1 & GD-2) and the second (GD-3 & GD-4) pairs of the GDs always are summed up along the axis $\mathrm{O_g}x_c^{\mathrm{g}}$. Sometimes only 3 executive devices are used.

At the GMC Z-arrangement on the SC body, when the axis $\mathrm{O_g}x_c^{\mathrm{g}}$ is the same as the axis $\mathrm{O}z$ of the BRF, for $\sigma = \pi/6$ and $\beta_p \in [-\pi/2, \pi/2]$ the following 4 efficient GMC configurations Z-I, I=$1 \div 4$ (GMC without GD-I) are possible on the basis of *only* 3 *active* GDs. These configurations are represented at nominal state in Fig. 3*b* (Z-4 or Z-3) and in Fig. 3*c* (Z-2 or Z-1). So, the GMC scheme in Fig. 3*a* is *fault-tolerant* under diagnostics of the faulted GD and the GMC reconfiguration by *passages* between configurations Z-I by some logic conditions.

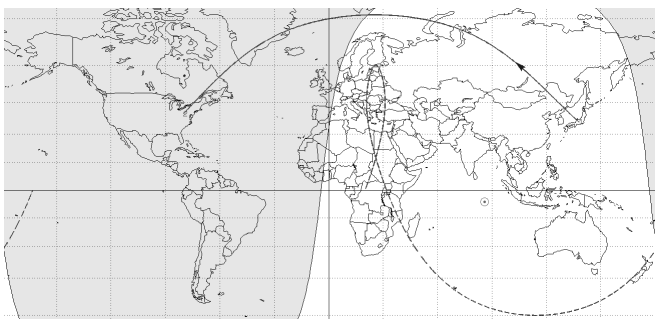

Fig. 4. Antenna pointing by the HEO spacecraft guidance

Fig. 5. Communication spacecraft *Sesat* with rotated SAPs

When a spacecraft is moving at a distant part of the high-elliptical orbit (HEO) by *Molniya* type (with apogee 46370 km and perigee 7370 km, Fig. 4) there are fulfilled sequence of the angular motion modes:

1° the SC antenna pointing to a given point at the Earth surface and then the target tracking during given time interval $\mathrm{T}_n \equiv [t_0^n, t_f^n]$;

2° the SC antenna guidance from any Earth point to next point during time $t \in \mathrm{T}_p \equiv [t_0^p, t_f^p]$, $t_f^p \equiv t_0^p + T_p$, where $T_p$ is given, see Fig. 4.

At the SC lifetime up to 15 years its structure inertial and flexible characteristics are slowly changed in wide boundaries, and the solar array panels (SAPs) are slowly rotated on the angle $\gamma(t) \in [0, 2\pi]$ with respect to the SC body for their tracking the Sun direction, see Fig. 5. Therefore at inertial matrix $\mathbf{A}^{\mathrm{o}}$ and partial frequencies $\Omega_j^q$ of the SC structure are not complete certain. Problems consist in

- synthesis of the SC antenna guidance laws for calculating $\boldsymbol{\Lambda}^p(t)$, angular rate $\boldsymbol{\omega}^p(t)$ and acceleration $\dot{\boldsymbol{\omega}}^p(t) = \boldsymbol{\varepsilon}^p(t)$ vectors of the SC body programmed motion by tasks 1°, 2°;
- dynamical design of *simple* and *reliable* GMC digital control law $\mathbf{u}_k^{\mathrm{g}} = \{u_{pk}^{\mathrm{g}}\}$ on discrete estimations $\hat{\boldsymbol{\Lambda}}_s$, $\hat{\boldsymbol{\omega}}_s$ and the GMC state vector $\boldsymbol{\beta}_k$ values when the SC structure characteristics are uncertain and its damping is very weak.

## 5. THE ANTENNA GUIDANCE LAWS

The analytic matching solution have been obtained for problem of the SC angular guidance at its antenna pointing to the Earth target and the same target tracking at time $t \in \mathrm{T}_n$ with $t_f^n \equiv t_0^n + T_n$. Solution is based on a vector composition of all elemental motions in the GRF $\mathbf{E}_{\mathrm{e}}$ using the HRF $\mathbf{E}_{\mathrm{e}}^{\mathrm{h}}$, the SRF $\boldsymbol{\mathcal{S}}$ and orthogonal matrix $\mathbf{C}_{\mathrm{h}}^{\mathrm{s}} \equiv \tilde{\mathbf{C}} = \| \tilde{c}_{ij} \|$ which defines the SRF $\boldsymbol{\mathcal{S}}$ orientation with respect to the HRF $\mathbf{E}_{\mathrm{e}}^{\mathrm{h}}$.

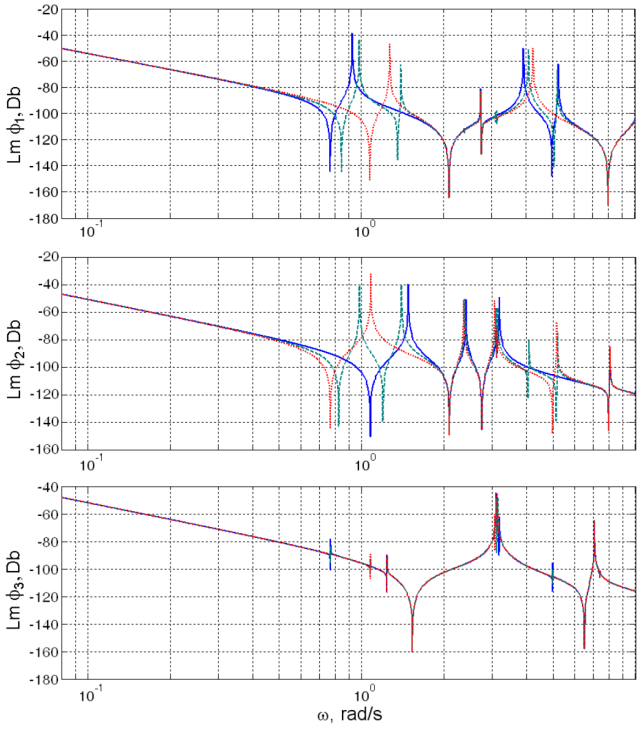


Fig. 6. The SC natural logarithmic amplitude frequency characteristics on the yaw ($\phi_1$), roll ($\phi_2$) and pith ($\phi_3$) channels for different SAPs' positions: for $\gamma = 0$ by entire blue line , for $\gamma = 45°$ by dotted green line and for $\gamma = 90°$ by pointed red line.

Normed to the communication oblique range D vector $\mathbf{v}$ and the SC body programmed angular rate vector $\boldsymbol{\omega}^p$ with respect the GRF $\mathbf{E}_e$ are presented in the SRF $\boldsymbol{\mathcal{S}}$ as $\mathbf{v}_e^s = \{\tilde{v}_{ei}^s, i = 1 \div 3\}$ and $\boldsymbol{\omega}_e^{sp} = \{\omega_{ei}^{sp}, i = 1 \div 3\}$. Calculation of vector $\boldsymbol{\omega}_e^{sp}$ is carried out by *explicit* analytical relations

$$\omega_{e1}^{sp} = -\frac{\tilde{v}_{e3}^s \tilde{c}_{21} + \tilde{v}_{e2}^s \tilde{c}_{31}}{2\tilde{c}_{11}};\ \omega_{e2}^{sp} = -\tilde{v}_{e3}^s;\ \omega_{e3}^{sp} = \tilde{v}_{e2}^s. \qquad (12)$$

By numerical solution of the quaternion differential equation $\dot{\boldsymbol{\Lambda}}_e^{sp} = \boldsymbol{\Lambda}_e^{sp} \circ \boldsymbol{\omega}_e^{sp}/2$ one can obtain values of vectors $\boldsymbol{\lambda}_{es}^{sp} \equiv \boldsymbol{\lambda}_e^{sp}(t_s)$ for the discrete time moments $t_s \in \mathrm{T}_n$ $\forall s = 0 \div n_q$, $n_q = T_n/T_q$ with period $T_q$ when initial value $\boldsymbol{\Lambda}_e^{sp}(t_0^n)$ is given.

Further solution is based on the elegant extrapolation of values $\boldsymbol{\sigma}_{es}^{sp} = \boldsymbol{\lambda}_{es}^{sp}/(1 + \lambda_{0\,es}^{sp})$ by the vector of Rodrigues' modified parameters and values $\boldsymbol{\omega}_{es}^{sp}$ by the angular rate vector. The extrapolation is carried out by these two sets of $n_q$ coordinated 3-degree vector splines with analytical obtaining a high-precise approximation of the SRF $\boldsymbol{\mathcal{S}}$ guidance motion with respect to the GRF $\mathbf{E}_e$ both on vector of angular acceleration and on vector of its local derivative. At last stage, required functions $\boldsymbol{\Lambda}^p(t)$, $\boldsymbol{\omega}^p(t)$, $\boldsymbol{\varepsilon}^p(t)$ and $\dot{\boldsymbol{\varepsilon}}^p(t) = \overset{*}{\boldsymbol{\varepsilon}}{}^p(t) + \boldsymbol{\omega}^p(t) \times \boldsymbol{\varepsilon}^p(t)$ is calculated by *explicit* formulas.

Fast onboard algorithms for the SC antenna guidance by its rotation maneuver into given time interval $t \in \mathrm{T}_p$ with restrictions to $\boldsymbol{\omega}^p(t)$ and $\dot{\boldsymbol{\omega}}^p(t)$ corresponding restrictions to $\mathbf{h}(\boldsymbol{\beta}(t))$ and $\dot{\boldsymbol{\beta}}(t)$ in a class of the SC angular motions, were elaborated. Here the boundary conditions on left ($t = t_0^p$) and right ($t = t_f^p$) trajectory ends are given as follows:

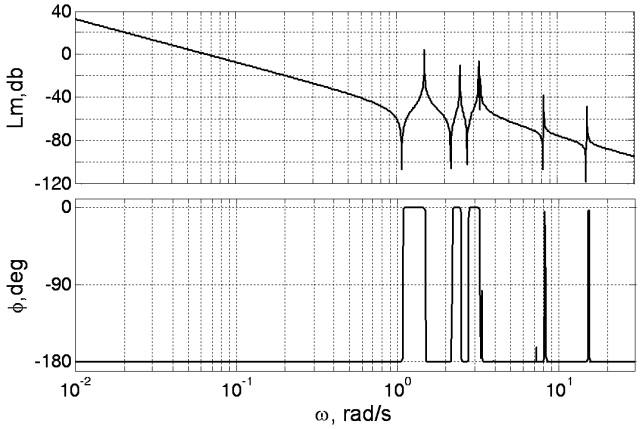


Fig. 7. The spacecraft natural logarithmic amplitude and phase frequency characteristics on the roll channel continuous open-loop

$$\boldsymbol{\Lambda}^p(t_0^p) = \boldsymbol{\Lambda}_0^p;\ \boldsymbol{\omega}^p(t_0^p) = \boldsymbol{\omega}_0^p;\ \boldsymbol{\varepsilon}^p(t_0^p) = \boldsymbol{\varepsilon}_0^p; \qquad (13)$$

$$\boldsymbol{\Lambda}^p(t_f^p) = \boldsymbol{\Lambda}_f^p;\ \boldsymbol{\omega}^p(t_f^p) \equiv \boldsymbol{\omega}_f^p;\ \boldsymbol{\varepsilon}^p(t_f^p) = \boldsymbol{\varepsilon}_f^p. \qquad (14)$$

Developed approach to the problem is based on necessary and sufficient condition for solvability of *Darboux* problem. Solution is obtained as result of composition by three *simultaneously* derived elementary rotations of embedded bases $\mathbf{E}_k$ about units $\mathbf{e}_k$ of *Euler* axes, $k = 1 \div 3$, which position is defined from the boundary conditions (13) and (14) for initial spatial problem. For all 3 elementary rotations with respect to units $\mathbf{e}_k$ the boundary conditions are analytically assigned. Into the IRF $\mathbf{I}_\oplus$ the quaternion $\boldsymbol{\Lambda}^p(t)$ is defined by the production

$$\boldsymbol{\Lambda}^p(t) = \boldsymbol{\Lambda}_0^p \circ \boldsymbol{\Lambda}_1^p(t) \circ \boldsymbol{\Lambda}_2^p(t) \circ \boldsymbol{\Lambda}_3^p(t), \qquad (15)$$

where $\boldsymbol{\Lambda}_k^p(t) = (\cos(\varphi_k^p(t)/2), \sin(\varphi_k^p(t)/2)\ \mathbf{e}_k)$, $\mathbf{e}_k$ is unit of *Euler* axis by $k$'s rotation, and functions $\varphi_k^p(t)$ present the elementary rotation angles in analytical form. These functions were selected in class of splines by 5 degree. Explicit time functions $\boldsymbol{\Lambda}^p(t)$, $\boldsymbol{\omega}^p(t)$ and $\boldsymbol{\varepsilon}^p(t)$ are applied at onboard computer for the time moments $t_s$ by the SC antenna guidance at its both pointing ($t_s \in \mathrm{T}_n$) and rotation maneuver ($t_s \in \mathrm{T}_p$).

## 6. THE STRUCTURE OSCILLATIONS

Presented in Somov (2002) and applied here the distribution law $f_\rho(\boldsymbol{\beta}) = 0$ of the GMC normed AM $\mathbf{h}(\boldsymbol{\beta}) = \Sigma\, \mathbf{h}_p(\beta_p)$ between GD's pairs ensures its singular state only at separate time moments and bijectively connects the vector $\mathbf{M}^{\mathbf{g}}(t)$ with vectors $\boldsymbol{\beta}(t)$ and $\dot{\boldsymbol{\beta}}(t) = \mathbf{u}^{\mathrm{g}}(t)$. Therefore for preliminary study it is rational to considerate the column $\mathbf{M}^{\mathbf{g}}(t) = \{\mathrm{M}_i^{\mathrm{g}}\}$ as control vector.

Applying the state vector $\mathbf{x} = \{\boldsymbol{\phi}, \mathbf{v}_\delta, \boldsymbol{\omega}, \dot{\mathbf{q}}, \mathbf{q}\}$ and denotations $\mathbf{u}(t) = \mathbf{M}^{\mathbf{g}}(t)$, $\mathbf{y}(t) = \boldsymbol{\phi}(t)$ for a linearizing procedure of the SC model (7) at neighbourhood of the SC equilibrium in the ORF $\mathbf{O}$ one can obtain standard continuous model $\dot{\mathbf{x}} = \mathbf{A}\mathbf{x} + \mathbf{B}\mathbf{u}$, $\mathbf{y} = \mathbf{C}\mathbf{x}$. Comparison of linear (8) and hysteresis (7) modelling of the SC structure weak-damped oscillations was developed by numerical methods.

The SC natural logarithmic frequency characteristics on the roll channel continuous open-loop are presented in Fig. 7 at linear modelling with decrement $\delta_j^q = 2\,10^{-3}$ for all tones. At hysteresis modelling the same "frequency

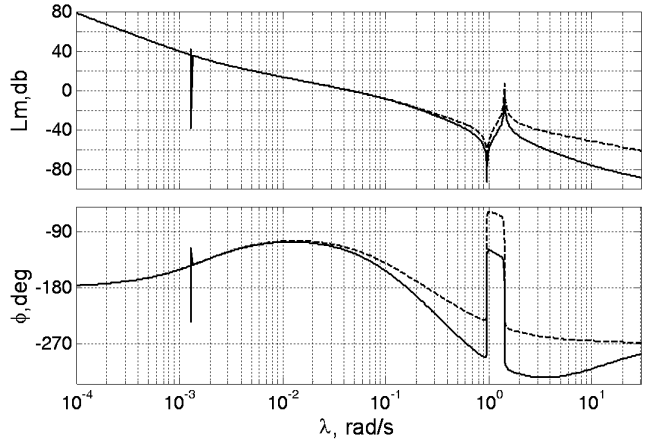


Fig. 8. The SC open-loop pseudo-frequency characteristics on roll channel: - - - - - without discrete filter, —— with discrete filter.

characteristics" were also computed by numerical simulation for a set of input command amplitudes. Obtained results are close, but resonance and anti-resonance "peaks" have very narrow form for hysteresis modelling, these differences are significant only for small input amplitudes.

## 7. FILTERING AND DIGITAL CONTROL

The error quaternion is $\mathbf{E}=(e_0,\mathbf{e})=\tilde{\mathbf{\Lambda}}^p(t)\circ\mathbf{\Lambda}$, the *Euler* parameters' vector $\boldsymbol{\mathcal{E}}=\{e_0,\mathbf{e}\}$, and the attitude error's matrix is $\mathbf{C}^e\equiv\mathbf{C}(\boldsymbol{\mathcal{E}})=\mathbf{I}_3-2[\mathbf{e}\times]\mathbf{Q}_e^{\mathrm{t}}$, where matrix $\mathbf{Q}_e\equiv\mathbf{Q}(\boldsymbol{\mathcal{E}})=\mathbf{I}_3e_0+[\mathbf{e}\times]$ with $\det(\mathbf{Q}_e)=e_0\neq 0$.

Let the GMC's required control torque vector $\mathbf{M}^{\mathrm{g}}$ (11) is formed as $\mathbf{M}^{\mathrm{g}}=\boldsymbol{\omega}\times\mathbf{G}^o+\mathbf{J}(\mathbf{C}^e\dot{\boldsymbol{\omega}}^p(t)-[\boldsymbol{\omega}\times]\mathbf{C}^e\boldsymbol{\omega}^p(t)+\mathbf{m}^{\mathrm{g}})$, where vector $\mathbf{m}^{\mathrm{g}}$ is a stabilizing component.

At given digital control period $T_u$ discrete frequency characteristics are computed via absolute pseudo-frequency $\lambda=2\mathrm{tg}(\omega T_u/2)/T_u$. For period's multiple $n_{\mathrm{q}}$ and a filtering period $T_q=T_u/\mathrm{n_q}$ applied filter have the discrete transfer function $\mathrm{W_f(z_q)}=(1+\mathrm{b}_1)/(1+\mathrm{b}_1\mathrm{z_q^{-1}})$, where coefficient $\mathrm{b}_1=-\exp(-T_q/T_{\mathrm{f}})$ and $\mathrm{z_q}=\exp(\mathrm{s}T_q)$.

By own absolute pseudo-frequency

$$\lambda_{\mathrm{q}}=(2/T_q)\mathrm{tg}(\omega T_q/2)=n_{\mathrm{q}}(2/T_u)\mathrm{tg}(\mathrm{arctg}(\lambda\, T_u/2)/n_{\mathrm{q}})$$

the discrete frequency characteristics $\tilde{\mathrm{W}}_{\mathrm{f}}(j\lambda_{\mathrm{q}})$ is presented as follows $\tilde{\mathrm{W}}_{\mathrm{f}}(j\lambda_{\mathrm{q}})=\mathrm{K}_{\mathrm{f}}^{\lambda}\ (j\lambda_{\mathrm{q}}-q_{\mathrm{q}}^{\lambda})/(j\lambda_{\mathrm{q}}-p_{\mathrm{q}}^{\lambda})$, where $\mathrm{K}_{\mathrm{f}}^{\lambda}=(1+\mathrm{b}_1)/(1-\mathrm{b}_1)$; $q_{\mathrm{q}}^{\lambda}=-(2/T_q)$ and $p_{\mathrm{q}}^{\lambda}=\mathrm{K}_{\mathrm{f}}^{\lambda}q_{\mathrm{q}}^{\lambda}$.

Discrete error quaternion and *Euler* parameters' vector are $\mathbf{E}_s=(e_{0s},\mathbf{e}_s)=\tilde{\mathbf{\Lambda}}^p(t_s)\circ\hat{\mathbf{\Lambda}}_s$ and $\boldsymbol{\mathcal{E}}_s=\{e_{0s},\mathbf{e}_s\}$, and the error filtering is executed by the relations

$$\tilde{\mathbf{x}}_{s+1}=\tilde{\mathbf{A}}\tilde{\mathbf{x}}_s+\tilde{\mathbf{B}}\mathbf{e}_s;\mathbf{e}_s^{\mathrm{f}}=\tilde{\mathbf{C}}\tilde{\mathbf{x}}_s+\tilde{\mathbf{D}}\mathbf{e}_s,\qquad(16)$$

where matrices $\tilde{\mathbf{A}},\tilde{\mathbf{B}},\tilde{\mathbf{C}}$ and $\tilde{\mathbf{D}}$ have diagonal form with $\tilde{a}_i=-\mathrm{b}_1^{\mathrm{f}}$; $\tilde{b}_i=\mathrm{b}_1^{\mathrm{f}}$; $\tilde{c}_i=-(1+\mathrm{b}_1^{\mathrm{f}})$ and $\tilde{d}_i=1+\mathrm{b}_1^{\mathrm{f}}$.

Applied stabilizing component $\mathbf{m}_k^{\mathrm{g}}$ is formed as follows:

$$\boldsymbol{\epsilon}_k=-2\mathbf{e}_k^{\mathrm{f}};\mathbf{g}_{k+1}=\mathbf{B}\mathbf{g}_k+\mathbf{C}\boldsymbol{\epsilon}_k;\mathbf{m}_k^{\mathrm{g}}=\mathbf{K}^{\mathrm{g}}(\mathbf{g}_k+\mathbf{P}\boldsymbol{\epsilon}_k).\quad(17)$$

Here matrices $\mathbf{B},\mathbf{C},\mathbf{P}$ and $\mathbf{K}^{\mathrm{g}}$ have diagonal form with

$$a_i=[(2/\mathrm{T}_u)\tau_{1i}-1]/[(2/\mathrm{T}_u)\tau_{1i}+1];$$
$$b_i=[(2/\mathrm{T}_u)\tau_{2i}-1]/[(2/\mathrm{T}_u)\tau_{2i}+1];$$
$$p_i=(1-b_i)/(1-a_i);\ c_i=p_i(b_i-a_i),$$

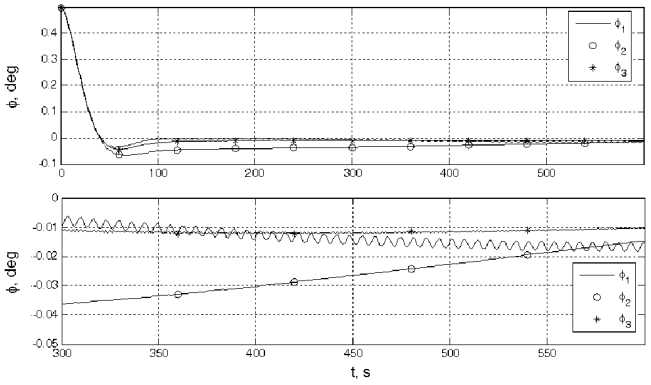


Fig. 9. Transient processes by attitude angles with respect to the ORF

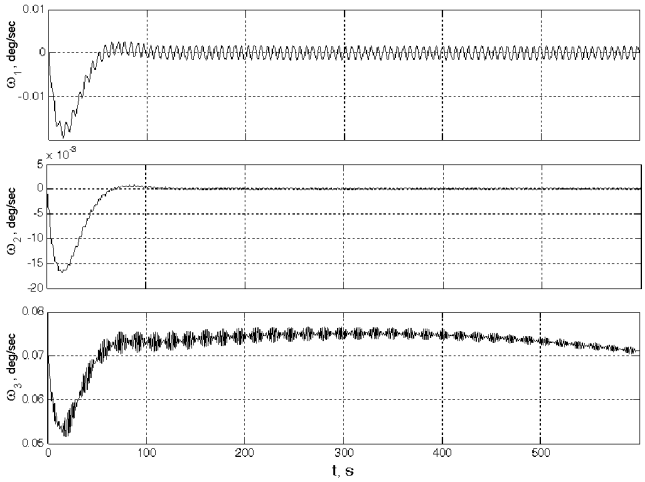


Fig. 10. Transient processes by angular rates

where $\tau_{1i},\tau_{2i}$ and $k_i^{\mathrm{g}}$ are pseudo-constant parameters which are selected and then turning (in progress of Somov (2001) and Somov (2007)) for ensuring the robust properties of gyromoment attitude control system by the flexible weak damping spacecraft. Only the SC attitude *filtered* error vector $\mathbf{e}_k^{\mathrm{f}}$ is applied for forming the stabilizing component $\mathbf{m}_k^{\mathrm{g}}$ (17).

The GMC's control torque is digitally formed by relation

$$\mathbf{M}_k^{\mathrm{g}}=\hat{\boldsymbol{\omega}}_k\times\hat{\mathbf{G}}_k^o+\hat{\mathbf{J}}(\mathbf{C}_k^e\boldsymbol{\varepsilon}_k^p-[\hat{\boldsymbol{\omega}}_k\times]\mathbf{C}_k^e\boldsymbol{\omega}_k^p+\mathbf{m}_k^{\mathrm{g}}),\qquad(18)$$

where $\hat{\mathbf{G}}_k^o=\hat{\mathbf{J}}\hat{\boldsymbol{\omega}}_k+\boldsymbol{\mathcal{H}}(\boldsymbol{\beta}_k)$, $\mathbf{C}_k^e=\mathbf{C}(\boldsymbol{\mathcal{E}}_k^{\mathrm{f}})$, $\boldsymbol{\varepsilon}_k^p=\dot{\boldsymbol{\omega}}^p(t_k)$ and $\boldsymbol{\omega}_k^p=\boldsymbol{\omega}^p(t_k)$. At last, the GMC digital control law $\mathbf{u}_k^{\mathrm{g}}$ is appeared from conditions

$$\mathbf{A}_{\mathrm{h}}(\boldsymbol{\beta}_k)\,\mathbf{u}_k^{\mathrm{g}}=-\mathbf{M}_k^{\mathbf{g}};\ \langle\partial f_\rho(\boldsymbol{\beta}_k)/\partial\boldsymbol{\beta},\mathbf{u}_k^{\mathrm{g}}\rangle=0.\qquad(19)$$

The filtering efficiency is demonstrated by pseudo-frequency characteristics in Fig. 8 for same the SC roll channel but by open-loop with digital control, when the control period $T_u=4$ s, the filtering period $T_q=1$ s and the time constant $T_{\mathrm{f}}=2$ s. Here is not stability on the channel without the discrete filter (16).

## 8. COMPUTER SIMULATION

A software system was applied for computer simulation and dynamic analysis of the flexible SC antenna pointing model (7) and (8) with discrete filtering (16), discrete control law (17), (18) and forming the GMC digital control (19). For considered variants of digital gyromoment control

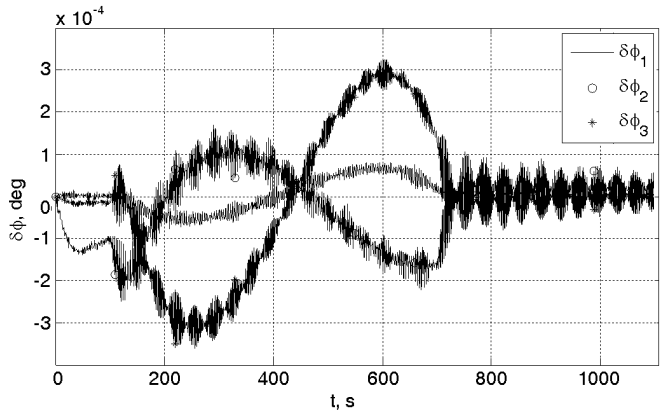


Fig. 11. The SC antenna oscillations at sequence of the guidance modes

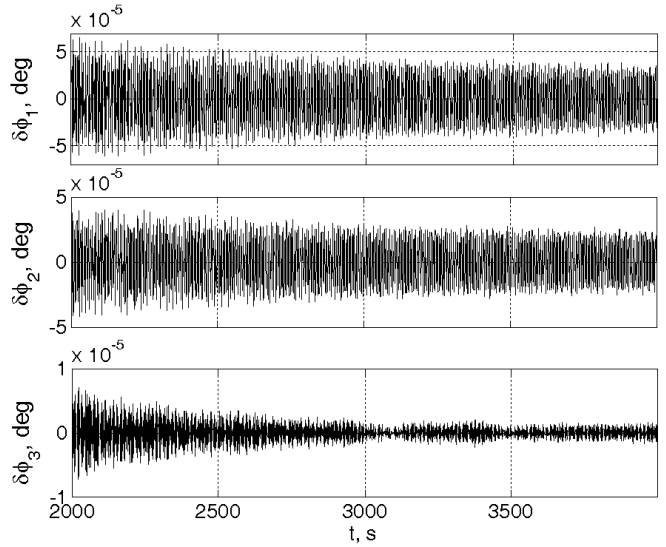


Fig. 12. The SC antenna's weak-damped oscillations at a longtime tracking

(see pseudo-frequency characteristics on the open-loop roll channel in Fig. 8) some results are presented in Fig. 9 and Fig. 10 on the SC attitude stabilization in the ORF **O** when for $t = t_0 = 0$ initial conditions on all variables are zero except $\phi_i(0) = 0.5$ deg for all $i = 1 \div 3$. Additional angular deflection by antenna's flexibility $\delta\boldsymbol{\phi}$ (9) are presented

- in Fig. 11 as sequence of the SC antenna guidance modes: 1° – pointing and target tracking, 2° – guidance by a rotation maneuver to next target and again 1° – the same next target tracking, see Fig. 4;
- in Fig. 12 – the antenna's weak-damped oscillations at a longtime tracking.

Numerical calculations prove that for small amplitude of the SC structure oscillations, results are significantly differ at linear and a hysteresis modelling of a weak structure damping.

## 9. CONCLUSIONS

New approach for modelling a physical hysteresis was developed and it application for digital gyromoment attitude control of a flexible spacecraft structure was considered. New results on the SC antennas' guidance, a digital gyromoment spacecraft attitude control and the flexible antennas fine pointing, were presented.

These results were also successfully applied for a space free-flying robot at transportation the flexible large-scale mechanical payload (Somov, 2006).

## REFERENCES


Kochneva, L. (1979). *Internal Friction in Solid Bodies at Oscillations*. Nauka, Moscow. In Russian.

Krasnosel'skii, M. and Pokrovskii, A. (1983). *Systems with a Hysteresis*. Nauka, Moscow. In Russian.

Palmov, V. (1976). *Oscillations of Flexible-plastic Bodies*. Nauka, Moscow. In Russian.

Panovko, Y. (1960). *Internal Friction at Oscillations of Flexible Systems*. Fizmatgiz, Moscow. In Russian.

Pisarenko, G. (1970). *Oscillations of Mechanical Systems with Regard for an Imperfect Flexibility of Materials*. Naukova Dumka, Kiyev. In Russian.

Somov, Y. (2000). Model of physical hysteresis and control of the image motion oscillations at a large space telescope. In *Proceedings of 2nd International Conference COC'2000*, volume 1, 70–75. Saint Petersburg.

Somov, Y. (2001). Robust stabilization of a flexible spacecraft at partial discrete measurement and a delay in forming control. *Journal of Computer and Systems Sciences International*, 40(2), 287–307.

Somov, Y. (2002). Methods and software for research and design of spacecraft robust fault tolerant control systems. In *Automatic Control in Aerospace 2001*, 28–40. Elsevier Science, Oxford.

Somov, Y. (2004). Modelling physical hysteresis and control of a fine piezo-drive. In *Proceedings of 1st IEEE/IUTAM International Conference "Physics and Control"*, volume 4, 1189–1194. Saint Petersburg.

Somov, Y. (2006). Analytic synthesis of a programme gyromoment conrol by free-flying space robot. *Conrol Problems*, (6), 72–78.

Somov, Y. (2007). Robust digital stabilization of a flexible spacecraft. In *Proceedings of the VI International conference "System Identification and Control Problems"*, volume 1, 264–292. Institute of Control Science, the Russian Academy of Siences, Moscow. In Russian.

Somov, Y., Butyrin, S., and Somov, S. (2005a). Coupling and damping the structure oscillations at spacecraft gyromoment digital control. In *Proceedings of the IEEE/EPS International conference "Physics and Control"*, 497–502. Saint Petersburg.

Somov, Y., Platonov, V., and Sorokin, A. (2005b). Steering the control moment gyroscope clusters onboard high-agile spacecraft. In *Automatic Control in Aerospace 2004. A proceeding volume from the 16th IFAC Symposium*, 137–142. Elsevier Ltd, Oxford.